ELSEVIER

Chemical Engineering Journal 141 (2008) 284–289

Chemical Engineering Journal

www.elsevier.com/locate/cej

Effect of carbon addition on the Pt-Sn/γ-Al_2O_3 catalyst for long chain paraffin dehydrogenation to olefin

Songbo He [a,b], Chenglin Sun [a,*], Hongzhang Du [a], Xihai Dai [b,c], Bin Wang [c]

[a] *Dalian Institute of Chemical Physics, Chinese Academy of Sciences, Dalian, Liaoning 116023, PR China*
[b] *Graduate University of Chinese Academy of Sciences, Beijing 100049, PR China*
[c] *PetroChina Fushun Petrochemical Company, Fushun, Liaoning 113001, PR China*

Received 19 September 2007; received in revised form 5 December 2007; accepted 28 December 2007

Abstract

Carbon-covered alumina (CCA) was prepared by the pyrolysis of the sucrose dispersed on a gamma alumina surface. BET, mercury porosimetry, SEM, XRD, H_2-chemisorption, CO-chemisorption, NH_3-TPD and TG-DTA were used for the carriers and the corresponding catalyst characterization. The results showed that the carbon of the CCA samples had negative influence on the catalytic initial activity of the Pt-Sn/CCA catalysts for the dehydrogenation of *n*-octadecane, but it was helpful to enhance the selectivity of the products and especially the stability of the catalysts markedly.

Keywords: Dehydrogenation; Carbon-covered alumina (CCA); Octadecane; Long chain paraffin; Pt-Sn catalysts

1. Introduction

In order to ease the energy shortage in the world, enhanced oil recovery (EOR) technology has attracted wide attention [1]. Anionic surfactants are widely used in EOR. Heavy alkylbenzene sulfonate (HABS) has been proved to be a kind of excellent anionic surfactants for its super performance in reducing the oil residual saturation through the reduction of interfacial tension (IFT) between oil and water phases [2]. HABS is produced by the sulfonation of heavy alkylbenzene (HAB). But as a by-product from linear alkylbenzene (LAB) synthesis [3], HAB cannot meet the practical demand. In addition, recent research showed that the ability to decrease crude oil/reservoir water interfacial tension of longer chain-length HABS (C_{16} and C_{18}) was markedly better than that of shorter chain-length (C_{12} and C_{14}) [4]. Therefore, a new technical route to produce HAB directly as a main-product has been explored: the longer chain normal paraffins (*n*-$C_{16–19}$) were dehydrogenated and then alkylated with benzene. But up to now, all the catalysts for the dehydrogenation of long chain paraffins were designed to produce the linear olefins for the manufacture of biodegradable detergents from the raw materials such as *n*-$C_{10–13}$ [5,6]. The catalysts might be deactivated by coke more easily during the dehydrogenation of *n*-$C_{16–19}$ due to the longer chain length. So the actual long chain paraffin dehydrogenation catalysts cannot meet the production needs, and the new catalysts for the dehydrogenation for $C_{16–19}$ should have higher catalytic stability.

It is well known that the best catalysts for the dehydrogenation of alkanes are generally supported Pt-Sn bimetallic catalysts [5,7]. Improvements in stability of the catalysts may be achieved by (i) changing the impregnation methods of tin, such as Pt–Sn complex method [8] and content of tin in the catalysts [9]. The addition of tin may act as a spacer or form the ensembles of a favorable size, and help migrate coke deposition on the active Platinum to the support surface [10]. And (ii) changing the type of support or modifying the properties of the support by the addition of another metal such as Zn and Mg to form spinel-type structures like zinc and magnesium aluminates which had high mechanical resistance and very low surface acidity [11–13].

Alumina is the most widely used support material for the dehydrogenation catalysts by reason of its superior capability to maintain a high degree of platinum dispersion which is essential for achieving high dehydrogenation activity [5]. But its strong acidity tends to cause the side reactions and coke formation [14]. Carbon is another widely used support material for catalysts, but it is not favorable for the dehydrogenation

* Corresponding author. Tel.: +86 411 84379133; fax: +86 411 84699965.
E-mail address: clsun@dicp.ac.cn (C. Sun).

1385-8947/$ – see front matter © 2008 Elsevier B.V. All rights reserved.
doi:10.1016/j.cej.2007.12.036

catalysts on account of its drawbacks such as microporous and poor mechanical properties [15]. Recently a novel material so-called carbon-covered alumina (CCA) has been developed [15–19]. The alumina surface is coated with a thin layer of carbon, in this way, the favorable carbon surface properties (low acidity and anti-coking performance) will combine with the advantages of the alumina (textural and mechanical features).

The present investigation was undertaken in order to compare the activity, selectivity and stability of the two kinds of catalysts (Pt-Sn/Al_2O_3 and Pt-Sn/CCA) for the dehydrogenation of *n*-octadecane and explore the feasibility of the new Pt-Sn/CCA catalysts for the dehydrogenation of long chain paraffins (*n*-$C_{16–19}$).

2. Experimental

2.1. CCA and catalyst preparation

Commercial γ-alumina (Finechem Co. RIDIC, diameter 1–2 mm, bulk density 0.33 g cm^{-3}) with a bimodal pore structure was used for the preparation of CCA and supported Pt-Sn catalysts. CCA was prepared by the pyrolysis of sucrose highly dispersed on the surface of alumina following the method proposed by Lin et al. [15]: first, sucrose/Al_2O_3 precursors were prepared by impregnating γ-Al_2O_3 with aqueous solutions containing sucrose. After drying at 90 °C overnight, the precursors were calcined at 600 °C in N_2 for 30 min. The carbon content of the CCA samples was determined gravimetrically from the weight loss within temperature interval 300–650 °C in thermogravimetry/differential thermal analysis (TG-DTA) and found to be 12.57%. Pt-Sn/Al_2O_3 and Pt-Sn/CCA catalysts were prepared by the method of co-impregnation of the support with aqueous solutions of precursors. All the catalysts had the same metal content: 0.5 wt.% Pt and 1.5 wt.% Sn. $H_2PtCl_6{\cdot}6H_2O$ and $SnCl_2{\cdot}2H_2O$ were used as precursor salts. The aqueous solutions of platinum–tin precursors and alumina (or CCA) were first left unstirred for 30 min and then gently heated at 60–70 °C in order to evaporate the excess liquid. The catalysts were dried at 120 °C overnight and finally calcined at 520 °C (Pt-Sn/Al_2O_3 in air and Pt-Sn/CCA in N_2) for 4 h.

2.2. Catalyst characterization

The carbon content of the CCA samples and used catalysts were measured by a TG-DTA instrument (SETSYS 16/18, France) from room temperature to 800 °C at a heating rate of 10 °C min^{-1} in an air flow of 50 ml min^{-1}; α-Al_2O_3 was used as a reference. The BET surface areas were calculated from the adsorption isotherms of nitrogen at 77 K on a volumetric adsorption system (Micromeritics ASAP 2010, American). All samples were degassed at 200 °C before BET measurements. Mercury porosimetry analysis was generated using a mercury porosimeter (Micromeritics Autopore 9520, American). Samples were outgassed in vacuum (0.01 Torr) for 1 h at 95 °C. An arbitrary mercury contact angle of 130° and a surface tension of 485 dynes/cm were used to calculate pore size distributions data from the mercury intrusion–extrusion curves. The morphology of the samples was examined under a scan electron microscope (KYKY-AMRAY-1000B, China) operated at an accelerating voltage of 25 kV. The crystallinity of the samples was analyzed by powder X-ray diffraction (Rigaku D/max-γB powder diffractometer, Japan) with Cu Kα radiation at 40 kV and 40 mA in the scan 2θ range of 10–80°. Pulse chemisorption of H_2 and CO experiments were performed to analyze the Pt dispersion of the catalysts (Micromeritics AutoChem II 2920, American). The samples were reduced under H_2 (99.99%, 20 ml/min) at 500 °C for 1 h, then purged in Ar (He for CO chemisorption) (99.99%, 20 ml/min) at 520 °C for 1 h and cooled down to 50 °C. The 0.1 cm^3 pulses of a mixture of 10% H_2 in Ar (5% CO in He for CO chemisorption) were sent to the reactor, and the time between pulses was 4 min. Temperature-programmed desorption of ammonia (NH_3-TPD) experiments were carried out to analyze the acidic properties of the catalysts (Micromeritics AutoChem II 2920, American). The samples were pretreated at 500 °C for 1 h under helium stream (20 ml min^{-1}). After cooling to 100 °C, NH_3 (99.96%) was adsorbed. The desorption was carried out with a temperature ramp of 10 °C min^{-1}, and the desorbed products were detected by a quadruple mass spectrometer.

2.3. Dehydrogenation of n-octadecane

A fixed bed micro-catalytic reactor was employed to carry out the dehydrogenation of *n*-octadecane, 2.5 ml of fresh catalysts were charged to the reactor. Prior to the dehydrogenation, the catalysts were reduced in H_2 flow (500 ml min^{-1}) for 2 h at 470 °C followed by cooling to the feed-in temperature (380 °C). A self-heated plunger metric pump was used to feed the reactant into the reactor. Then the temperature was programmed up to the reaction temperature within 60 min. The reaction conditions were: reaction temperature = 455 °C, pressure = 0.14 MPa, hydrogen flow rate = 500 ml min^{-1}, *n*-octadecane flow rate = 50 ml h^{-1}. The purity of hydrogen gas was 99.99% or more. The reactant (*n*-octadecane) was industry grade from Cangzhou Jincang Chemical Corporation Limited (Hebei, China) and the total normal paraffins (TNP) is 97.2%. The reactant was analyzed by GC-MS (Finnigan Polaris Q, American) and the composition was given in Table 1.

The bromine number of the effluents was determined by the UOP laboratory test methods (UOP 304-90) [20] and the conversion of *n*-octadecane was calculated as the multiplication of 1.57 and bromine number. The diolefins content were analyzed by GC (Agilent-6890N/5973, American) equipped with flame ionization detector (FID) using a HP-FFAP column (30 m × 0.53 mm × 1.0 μm, Agilent, American). And the aromatics were determined by GC (Agilent-6890N/5973, American) equipped with FID using a HP-PONA column

Table 1
Composition of the reactant (*n*-C18 paraffin)

n-C_{16}	*n*-C_{17}	*n*-C_{18}	*n*-C_{19}	*n*-C_{20}	Alkyl-halides
2.27%	0.13%	88.88%	0.04%	0.18%	5.84%

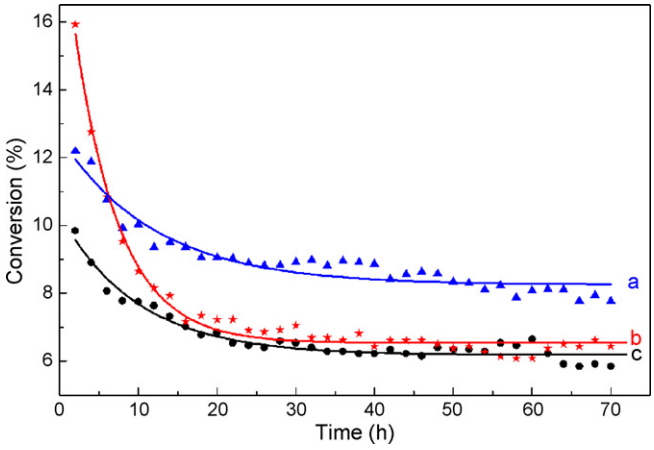

Fig. 1. Dependence of the dehydrogenation activity of (a) Pt-Sn/CCA, (b) Pt-Sn/Al_2O_3 and (c) DHE-7(UOP) catalysts for *n*-octadecane on reaction time.

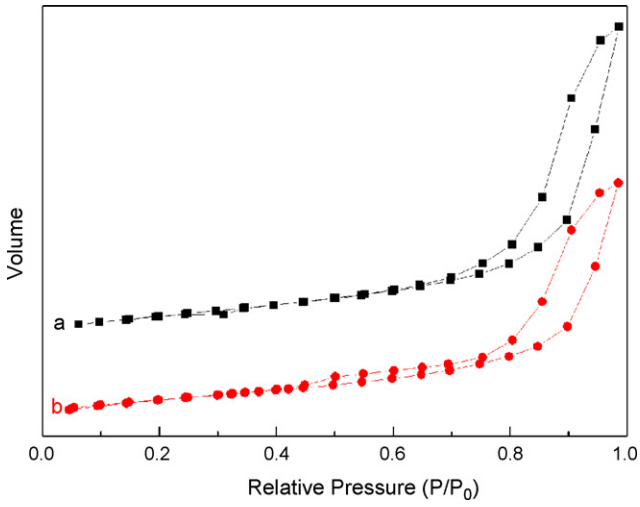

Fig. 2. Nitrogen adsorption/desorption isotherms of (a) Al_2O_3 and (b) CCA samples.

(100 m × 0.25 mm × 0.5 μm, Agilent, American). The selectivity is defined as the fraction of mono-olefins in total olefins of the effluents.

3. Results and discussion

3.1. Catalytic properties of Pt-Sn/Al_2O_3 and Pt-Sn/CCA catalysts

The catalytic activity and stability of the dehydrogenation of *n*-octadecane over Pt-Sn/CCA, Pt-Sn/Al_2O_3 and commercial DEH-7 (UOP) catalysts are depicted in Fig. 1. As can be seen from it, the catalytic activity and stability of the DEH-7 catalysts are not satisfactory. The Pt-Sn/Al_2O_3 catalysts, over which the conversion of *n*-octadecane during the first hour reached 15.9%, performed the highest catalytic initial activity. Although, the Pt-Sn/CCA catalysts exhibited a bit lower catalytic initial activity (12.2%), they showed better stability with respect to the reaction time than that of Pt-Sn/Al_2O_3 catalysts. The Pt-Sn/Al_2O_3 catalysts lost their activity very rapidly during the earlier 20 h successive reaction, and maintained their activity (the conversion is about 6.5%) over a comparatively extended period of time thereafter. However, the Pt-Sn/CCA catalysts retained a stable state (the conversion is about 8.5%) after 10 h on stream.

The product distributions of the dehydrogenation of *n*-octadecane over different catalysts are shown in Table 2. It can be observed that the diolefin content of the dehydrogenation products over the Pt-Sn/CCA catalysts was relatively lower than that over the Pt-Sn/Al_2O_3 catalysts, and aromatics of the effluents were scarcely observed. This fact indicated that the deep dehydrogenation reaction over the Pt-Sn/CCA catalysts was prevented more efficiently than that over the Pt-Sn/Al_2O_3 catalysts.

3.2. Texture and surface properties of Al_2O_3 and CCA samples

3.2.1. BET and mercury porosimetry analysis

The physico-chemical characterization data of the alumina and CCA samples are displayed in Table 3. It was reported that sucrose can be dispersed onto the surface of alumina [21]. Nitro-

Table 2
The products of the dehydrogenation of *n*-octadecane over different catalysts

Catalysts	Mono-olefins (wt.%)	Diolefins (wt.%)	Aromatics (wt.%)	Selectivity (%)
DEH-7(UOP)	8.46	1.38	Not detected (<50 ppm)	85.98
Pt-Sn/γ-Al_2O_3	10.37	2.43	Not detected (<50 ppm)	81.02
Pt-Sn/CCA	9.96	1.45	Not detected (<50 ppm)	87.29

Table 3
Texture of alumina and CCA samples

Carriers	S_{BET} (N_2) ($m^2\ g^{-1}$)	Pore volume ($cm^3\ g^{-1}$)	Vol.% in pores of diameter (nm)							
			<10	10–20	20–50	50–100	100–500	500–1000	1000–2000	>2000
γ-Al_2O_3	178.7	1.4999	4.66	29.43	10.81	3.32	7.19	14.57	26.47	3.55
CCA	191.2	1.2731	3.37	27.73	10.67	3.64	8.15	19.09	23.71	3.64

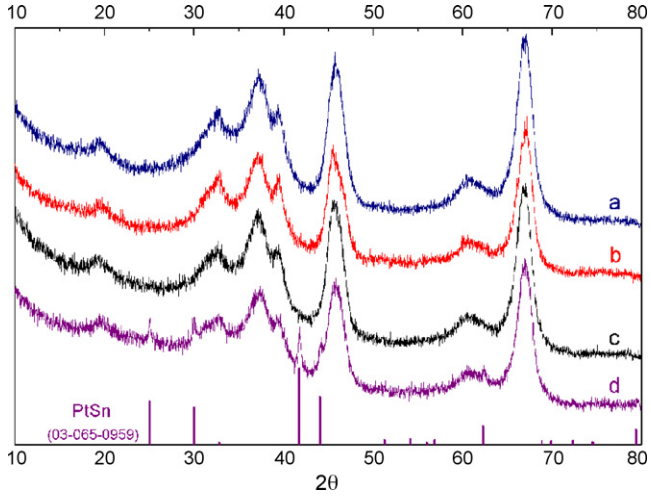

Fig. 3. XRD patterns of (a) γ-Al_2O_3, (b) Pt-Sn/γ-Al_2O_3, (c) CCA and (d) Pt-Sn/CCA.

gen adsorption/desorption isotherms (Fig. 2) for the alumina and CCA samples are of type IV [22], exhibiting H1 hysteresis loops characteristic of solids consisting of particles forming cylindrical channels of mesopore range. After the carbon deposition, a new capillary step appeared at a partial pressure (0.4–0.7) accompanied by the disappearance at a lower P/P_0 (0.2–0.4), which implied a new type of pore appeared in the CCA samples and some of the micropores of alumina disappeared. According to the XRD results (Fig. 3) which showed there were no crystalline sucrose and ordered carbon structures in the CCA samples, these new small pores would be attributed to the carbon formed by the pyrolysis of the sucrose [15]. The corresponding mercury pore size distributions of alumina and CCA samples are listed in Table 3. It was no surprise to find the decrease in pore volume after the carbon deposition. This did not imply a volume-filling process by carbon but rather a pore-blocking action, isolating regions of porosity [23]. And the carbon deposition was expected to narrow or shift median pore size to smaller value.

3.2.2. *SEM of the carriers*

The morphologies of the Al_2O_3 and CCA samples are shown in Fig. 4. After carbon covered on the surface of the alumina, the morphology changed greatly. Apparently, the carbon deposited as a monolayer or epitaxial multilayer patches, and parts of the carbon laid down as small hemispherical particles (or amorphous carbon). The carbon was comparatively uniformly covered on the alumina surface. According to Vissers's theory [17], the surface of the CCA samples would surpass that of the Al_2O_3 samples, which was in agreement with the results of the BET.

3.2.3. *Thermal analysis of the CCA samples*

The thermal analysis (TG and DTG) of the CCA samples is given in Fig. 5. The DTG curves showed a peak at around 100 °C due to the physically adsorbed water in the CCA samples [24] and a bigger endothermic signal at 475 °C, which

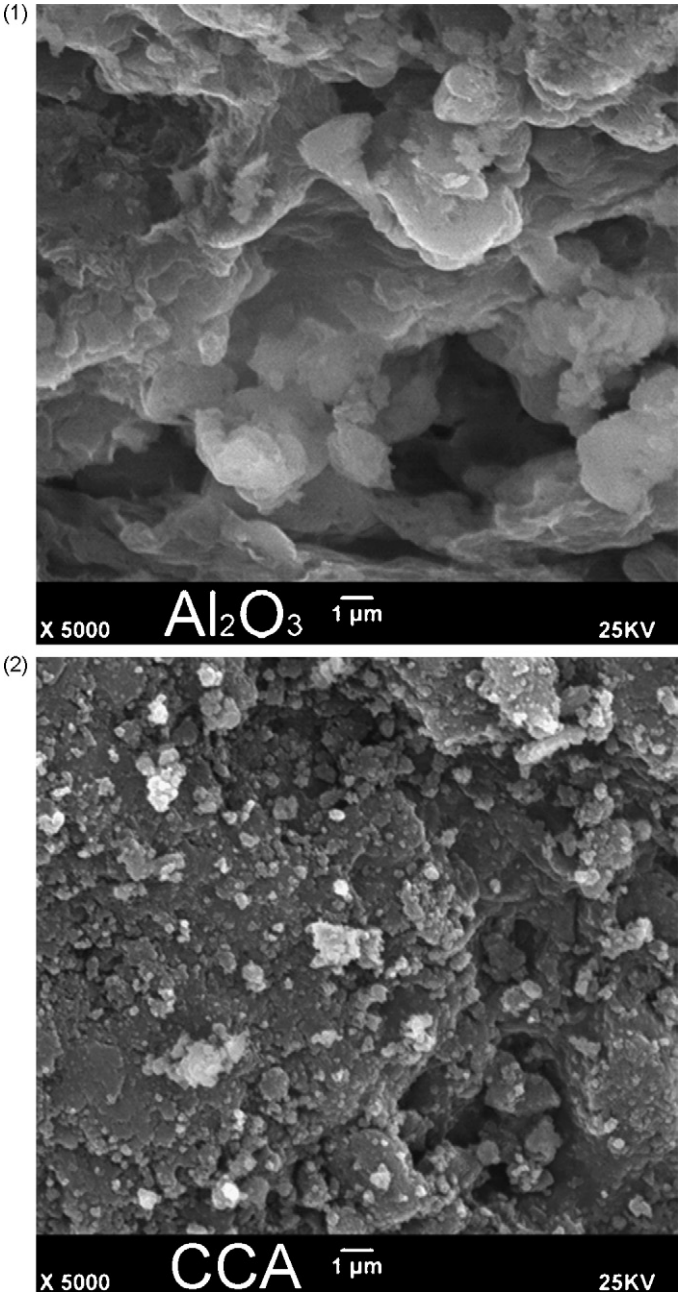

Fig. 4. SEM morphologies of Al_2O_3 and CCA samples.

would be attributed to the burning of the carbon on the CCA samples. The oxidation started at 300 °C and proceeded in one step in a narrow temperature interval which implied that the destruction of a single carbon phase occurred [25]. The carbon burned at this temperature region may have a higher ratio of H/C [26] and contain more polymerized/condensed carbon species [27].

From what has been discussed above, a conclusion may be arrived that the surface and pore structure of the carriers were changed after the carbon deposition. And these changes would have no or slight influence on the ability of large molecules to gain access into the catalysts [23].

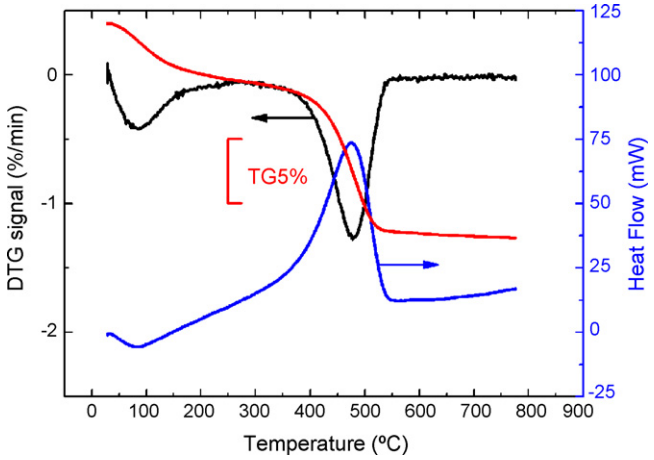

Fig. 5. TG/DTG-TA of CCA samples.

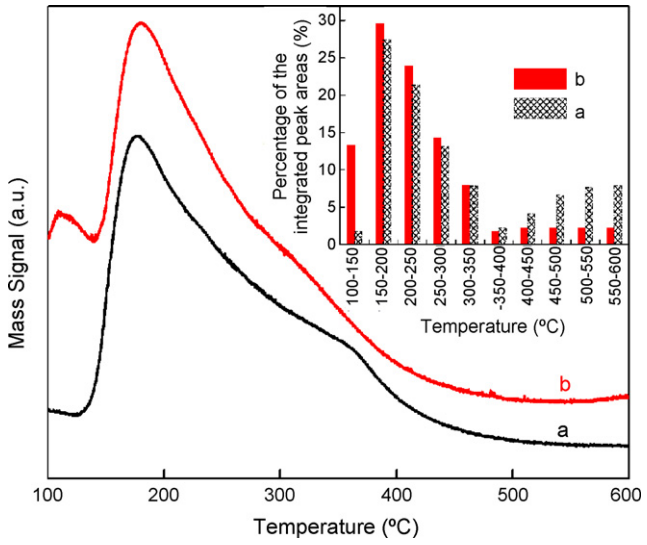

Fig. 6. NH_3-TPD profiles and the acidic strength distributions of (a) Pt-Sn/γ-Al_2O_3 and (b) Pt-Sn/CCA catalysts.

3.3. Characterization of the catalysts

3.3.1. X-ray diffraction spectra and pulse chemisorption of hydrogen

The Pt-Sn/Al_2O_3 and Pt-Sn/CCA catalysts after reduction were investigated by X-ray diffractometer in order to investigate any possible alloy formation between Pt and Sn and the results are also drawn in Fig. 3. XRD showed no lines attribute to a new Pt–Sn alloy, Pt or Sn phase for Pt-Sn/Al_2O_3 catalysts, and the new small peaks in the XRD pattern of Pt-Sn/CCA sample ($2\theta = 25°$, 30°, 41.8°, 44.3°, 62.3°, and 79.5°) indicated small amount of Pt-Sn alloy was formed on the CCA surface. The difference in alloy formation between Al_2O_3 supported and CCA supported Pt–Sn systems may come from the strong interaction between Al_2O_3 and Sn (II) [28].

Platinum dispersion estimated, which was calculated from the pulse chemisorption of hydrogen and CO at 50 °C using the assumption H(CO):Pt = 1 [29], are listed in Table 4. There is a close agreement between the results obtained by each method. This also agrees with the accepted concept that CO or H_2 chemisorption can be used to measure the metallic dispersion and calculate the Pt particle size on Pt-based catalysts [30]. Compared to the Pt-Sn/Al_2O_3 catalysts, a sharp decrease in platinum dispersion in the Pt-Sn/CCA catalysts was observed. It could be caused by the formation of small amount Pt-Sn alloy in the Pt-Sn/CCA catalysts according to the XRD results. Although, the support surface area could lead to different metal dispersions [31], it should not be considered as a unique factor in this analysis. And the hydrogen spillover on the Pt-Sn/Al_2O_3 catalysts of which the platinum dispersion exceeded 100% should also be considered [32].

Table 4
Characterization of Pt-Sn/Al_2O_3 and Pt-Sn/CCA catalysts

Catalysts	Pt dispersion (%)		NH_3 desorption (a.u. g^{-1})
	H_2 chemisorption	CO chemisorption	
Pt-Sn/γ-Al_2O_3	104.1	90.2	1.7
Pt-Sn/CCA	40.7	37.7	1.4

Previous studies had proved that the active site for the dehydrogenation of long chain paraffins to mono-olefins was the single platinum atom [33], and the platinum dispersion may be responsible for the initial reactivity indicated by Fig. 1.

3.3.2. Temperature-programmed desorption of ammonia

The temperature-programmed desorption profiles of ammonia adsorbed on Pt-Sn/Al_2O_3 and Pt-Sn/CCA catalysts are depicted in Fig. 6. On Pt-Sn/Al_2O_3 catalysts, a broad desorption peak with a maximum at about 175 °C and a shoulder at higher temperature (above 350 °C) could be clearly visible. The desorption peak at 175 °C of NH_3 on Pt-Sn/CCA was the same as that of Pt-Sn/Al_2O_3. But the higher temperature (350 °C) peak for the Pt-Sn/CCA catalysts was ambiguous and much smaller than that for the Pt-Sn/Al_2O_3 catalysts. It was noteworthy that the Pt-Sn/CCA catalysts had a remarkable low-temperature peak (100–140 °C). The acidic strength distributions of the two catalysts, estimated by the integrating the area of NH_3 desorption peaks, are also pictured in Fig. 6. It may be noted that the two catalysts showed wide acid strength distributions. According to the literature [34], the low-temperature peak can be ascribed to weak and medium strength acid sites, whereas the peak above 350 °C is typical of strong acidity. The carbon of the CCA samples led to a moderate decrease on the total acidity of the catalysts, as is listed in Table 4. And both weak–medium and strong acid sites were also affected by the carbon. It seemed that the deposited carbon helped the transference from the stronger acidic centers to the weaker ones.

It is accepted that Pt-Sn/Al_2O_3 catalyst is a kind of bifunctional catalyst, and the side reactions of the dehydrogenation such as isomerization and dehydrocyclization may occur on the acid sites. If there are excess acid sites, especially the strong acidity sites, the olefins will move to the acid sites to induce the side reactions and finally the formation of the carbonaceous deposit (commonly named coke). Elimination of acidic sites during catalyst preparation is one way of suppressing undesired reactions

Table 5
Carbon content of the fresh and used catalysts

Catalysts	Fresh (wt.%)	Carbon increased (wt.%)	
		Reaction time (6 h)	Reaction time (70 h)
Pt-Sn/γ-Al_2O_3	0	8.98	12.95
Pt-Sn/CCA	12.57	4.74	10.03

[14] and the enhanced stability and selectivity for Pt-Sn/CCA catalysts would be related to the comparatively weaker acidity and the acidic strength distributions.

3.3.3. Coke analysis

The data of carbon increased (coke formed) during the dehydrogenation reaction lasted for 6 and 70 h over Pt-Sn/Al_2O_3 and Pt-Sn/CCA catalysts are collected in Table 5. The coke on the Pt-Sn/CCA catalysts during the dehydrogenation reaction was far smaller than that on the Pt-Sn/Al_2O_3 catalysts, which also proved the viewpoint that carbon materials had a good anti-coking performance [35]. Coke may physically block active sites resulting in the loss of activity and deposit on the support [36]. During the initial stage of the reaction, the coke formation was very quick. It is easy to understand that a much higher dehydrogenation activity tends to dehydrogenating the olefins deeply. The coke formation is an accumulative process. With the prolongation of the reaction time, an increase of coke was observed, and simultaneously the velocity of carbon formation became slower. It seemed that the presence of carbon on the CCA could suppress the formation and accumulation of coke.

Coke deposition is an important factor of catalyst deactivation for the process of the dehydrogenation [10] and the improved stability for the Pt-Sn/CCA catalysts would be related to the low amount of coke over the catalysts.

4. Conclusions

It can be concluded that carbon addition on the Pt-Sn/γ-Al_2O_3 catalyst for long chain paraffin dehydrogenation had a remarkable role in increasing the stability of the catalysts. Although, the initial conversion over the Pt-Sn/CCA catalysts was a bit lower due to the depressed platinum dispersion which may be attributed to the small amount of Pt-Sn alloy formation in the Pt-Sn/CCA catalysts. The enhancement of the stability may be stimulated by the following factors: the carbon of the CCA samples changed the acidic strength distributions of the catalysts which also improved the selectivity of the products, and helped to prevent the coke formation and accumulation during the dehydrogenation reaction process.

Acknowledgments

The authors would like to acknowledge the contributions made by Yanli He, Shuanghe Meng and Changhai Xu in catalyst characterization measurements.

References

[1] J.J. Taber, Pure Appl. Chem. 52 (1980) 1323.
[2] Y. Zhang, G.Y. Zhang, P.W. Wang, J.P. Niu, J.C. Guan, H.X. Gu, Acta Phys-Chim Sin. 21 (2005) 161.
[3] J.A. Kocal, B.V. Vora, T. Imai, Appl. Catal. A 221 (2001) 295.
[4] J. Qu, Y. Zhu, Z. Sui, G. Zhou, Q. Zhang, Chem. Ind. Eng. Prog., China 22 (2003) 126.
[5] M.M. Bhasin, J.H. McCain, B.V. Vora, T. Imai, P.R. Pujado, Appl. Catal. A 221 (2001) 397.
[6] Imai Tamotsu, Abrevaya Hayim, US patent 4,595,673, 1986.
[7] P. Meriaudeau, Y. BenTaarit, A. Thangaraj, J.L.G. Almeida, C. Naccache, Catal. Today 38 (1997) 243.
[8] Y.J. Lei, Appl. Catal. 72 (1991) 33.
[9] W.S. Yang, L.W. Lin, Y.N. Fan, J.L. Zang, Catal. Lett. 12 (1992) 267.
[10] Z.S. Xu, T. Zhang, Y.N. Fang, L.W. Lin, Spillover and Migration of Surface Species on Catalysts, Elsevier Science Publ BV, Amsterdam, 1997, p. 425.
[11] G. Aguilarrios, M.A. Valenzuela, H. Armendariz, P. Salas, J.M. Dominguez, D.R. Acosta, et al., Appl. Catal. A 90 (1992) 25.
[12] M.A. Valenzuela, P. Bosch, G. Aguilarrios, B. Zapata, C. Maldonado, I. Schifter, J. Mol. Catal. 84 (1993) 177.
[13] W. Dong, H. Wang, Nat. Gas Chem. Ind., China 24 (1999) 9.
[14] O.A. Barias, A. Holmen, E.A. Blekkan, J. Catal. 158 (1996) 1.
[15] L. Lin, W. Lin, Y.X. Zhu, B.Y. Zhao, Y.C. Xie, G.Q. Jia, Langmuir 21 (2005) 5040.
[16] S.L. Butterworth, A.W. Scaroni, Appl. Catal. 16 (1985) 375.
[17] J.P.R. Vissers, F.P.M. Mercx, S.M.A.M. Bouwens, V.H.J.d. Beer, R. Prins, J. Catal. 114 (1988) 291.
[18] L.F. Sharanda, Y.V. Plyuto, I.V. Babich, Y.A. Babich, J.A. Moulijn, Mendeleev Commun. 3 (1999) 95.
[19] I.V. Plyuto, A.P. Shpak, J. Stoch, L.F. Sharanda, Y.V. Plyuto, I.V. Babich, et al., Surf. Interface Anal. 38 (2006) 917.
[20] Universal Oil Products, UOP Laboratory Test Methods for Petroleum and Its Products, Des Plaines, IL, 1992, pp. 304–390.
[21] Y. Xie, Y. Tang, Adv. Catal. 37 (1990) 1.
[22] L.D. Sharma, M. Kumar, A.K. Saxena, M. Chand, J.K. Gupta, J. Mol. Catal. A 185 (2002) 135.
[23] J. Baumgart, Y. Wang, W.R. Ernst, J.D. Carruthers, J. Catal. 126 (1990) 477.
[24] G.K. Reddy, K.S.R. Rao, P.K. Rao, Catal. Lett. 59 (1999) 157.
[25] L.F. Sharanda, Y.V. Plyuto, I.V. Babich, I.V. Plyuto, A.P. Shpak, J. Stoch, et al., Appl. Surf. Sci. 252 (2006) 8549.
[26] J. Chen, S. Lu, J. U. Petrol, China 23 (1999) 89.
[27] S.K. Sahoo, P.V.C. Rao, D. Rajeshwer, K.R. Krishnamurthy, I.D. Singh, Appl. Catal. A 244 (2003) 311.
[28] C. Kappenstein, M. Guérin, K. Lázár, K. Matusek, Z. Paál, J. Chem. Soc., Faraday Trans. 94 (1998) 2463.
[29] J. Freel, J. Catal. 25 (1972) 149.
[30] C.L. Pieck, C.R. Vera, J.M. Parera, G.N. Gimenez, L.R. Serra, L.S. Carvalho, et al., Catal. Today 107–108 (2005) 637.
[31] S.A. Bocanegra, A. Guerrero-Ruiz, S.R. de Miguel, O.A. Scelza, Appl. Catal. A 277 (2004) 11.
[32] P. Praserthdam, P. Choungchaisukasam, S. Assabumrungrat, T. Mongkhonsi, J. China Inst. Chem. Eng. 32 (2001) 143.
[33] T.L. Krylova, N.V. Nekrasov, B.S. Gudkov, V.R. Gurevich, S.L. Kiperman, Kinet. Catal. (Engl. Transl.) 21 (1981) 1060.
[34] S. Narayanan, A. Sultana, Q.T. Le, A. Auroux, Appl. Catal. A 168 (1998) 373.
[35] P.M. Boorman, K. Chong, Appl. Catal. A 95 (1993) 197.
[36] L.W. Lin, T. Zhang, J.L. Zang, Z.S. Xu, Appl. Catal. 67 (1990) 11.